# Proton Capture Dynamics in Quinoline Photobases: Substituent Effect and Involvement of Triplet States

Eric William Driscoll, Jonathan Ryan Hunt, and Jahan M. Dawlaty*[ID]

Department of Chemistry, University of Southern California, Los Angeles, California 90089, United States

S *Supporting Information*

ABSTRACT: Converting light into chemical energy often occurs through redox reactions that require transfer of several electrons and protons. Using light to control proton transfer has the potential for driving otherwise unfavorable protonation reactions or producing transient pH changes. Photoacids and photobases are fundamental functional elements that could serve this purpose. Previously, we have reported the thermodynamic drive for proton removal in a series of quinoline photobases using Forster cycle analysis of the singlet states. Because the existence of thermodynamic drive does not imply that the molecules can indeed capture protons in the excited state, in this work we report the kinetics of proton removal from water by 5-R-quinolines, R = {NH$_2$, OCH$_3$, H, Cl, Br, CN}, using ultrafast transient absorption spectroscopy. We found that the time constants and mechanisms of proton capture from water are highly sensitive to the substituent. In some cases, proton transfer occurs within the singlet manifold, whereas in some others intersystem crossing competes with this process. We have evidence that the triplet states are also capable of proton capture in two of the compounds. This renders the excited state proton transfer process more complicated than can be captured by the linear free energy relationships inferred from the energetics of the singlet states. We have measured proton capture times in this family to be in the range of several tens of picoseconds with no discernible trend with respect to the Hammett parameter of the substituents. This wide range of mechanisms is attributed to the high density of excited electronic states in the singlet and triplet manifolds. The ordering between these states is expected to change by substituent, solvent, and hydrogen bonding, thus making the rate of intersystem crossing and proton transfer very sensitive to these parameters. These results are necessary fundamental steps to assess the capabilities of photobases in prospective applications such as photomediated proton removal in redox reactions, steady state optical regulation of local pH, and pOH jump kinetics experiments.
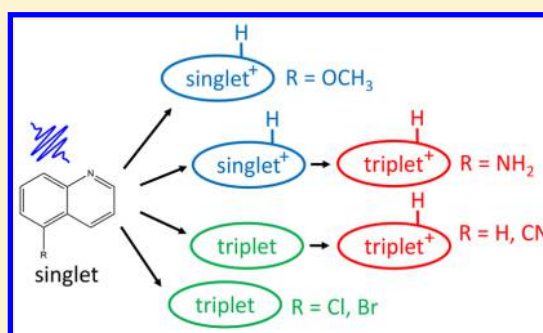
INTRODUCTION

Control over proton transfer is of primary importance in a wide range of chemical scenarios. Optical control of proton transfer may be achieved in molecules that change their acidity in the excited state. Photoacids are molecules that become significantly more acidic upon absorption of light and therefore serve as agents that can control local proton concentrations with light.[1−5] They have been widely used in a range of applications, including studying catalytic mechanisms,[6] protein folding,[7] and optical regulation of enzymatic activity.[8]

Despite the large body of literature on photoacids, there remains a significant lack of work on their counterparts, photobases, which are molecules that undergo an increase in pK_a upon light absorption. A few notable examples of photobases are quinoline,[9,10] acridine orange,[11] 3-styrylpyridine,[12] and xanthone.[13] Recently, we reported a systematic study of the thermodynamic drive for proton removal in the excited state (pK_a*) of a series of 5-substituted quinolines using Förster cycle analysis based on singlet states.[14] However, the existence of the thermodynamic drive for proton transfer in a singlet state does not account for relaxation via intersystem crossing or imply that deprotonation by a photobase is

kinetically feasible at all. Therefore, in this study, we investigate the effects the substituents have on the kinetics of proton transfer. In particular, we show that several competing relaxation pathways exist in the excited states of quinolines, some of which are capable of proton transfer as expected whereas others are not.

Previously, it has been observed that quinoline undergoes an excited state proton transfer reaction, acting as a Brønsted−Lowry base, accepting a proton from water, thus generating a hydroxide ion. There are some studies on the dynamics of substituted quinolines in aqueous media,[15−17] but none that investigate the effects of substituents' electron-donating/withdrawing capabilities (Hammett parameter[18,19]) in a systematic way. This sensitivity of photobasicity to substituents is the subject of this paper.

It is reasonable to hypothesize that a relationship between the thermodynamic drive (i.e., pK_a* as inferred from the Förster cycle[20,21] based on singlet states) and the rate of proton

transfer exists. Therefore, strongly electron-donating substituents, which result in a larger pK_a^*, will also result in a faster rate of proton capture in the excited state. However, it is known that triplet states have a significant role in the photophysics of quinolines.[22−26] We find that the relative energies of triplet states and the intersystem crossing rates are sensitive to the substituents. This renders the excited state proton transfer process more complicated than can be captured by the linear free energy relationships inferred from the energetics of the singlet states. This is in contrast to the structurally similar photoacid family of 1-naphthols, for which triplet states do not play a role and a correlation between thermodynamic drive and proton transfer rate has been reported.[27] Interestingly, we provide evidence that, in some cases, triplet states can undergo proton transfer. Because triplet states have longer lifetimes, this finding will be important for chemical applications of photobases which require a sustained pOH jump.

Similarly to photoacids that have been used to study catalysis mechanisms, protein folding dynamics, and enzyme activity regulation, we envision photobases to be another tool in studies that would require optical control over proton removal. We hope that elucidating these fundamental excited state processes in quinolines will allow photobases to become functional moieties in catalytic systems that require photomediated removal of protons.

◼ EXPERIMENTAL SECTION

Materials. 5-Aminoquinoline (NH$_2$Q), 5-methoxyquinoline (MeOQ), 5-bromoquinoline (BrQ), and 5-cyanoquinoline (CNQ) were purchased from Combi-Blocks. Quinoline (Q) and 5-chloroquinoline (ClQ) were purchased from Sigma-Aldrich. All compounds were used without further purification.

Steady State Spectroscopy. Absorption spectra were obtained using a Cary 50 UV−vis spectrophotometer. Emission spectra were collected on a Jobin-Yvon Fluoromax 3 fluorometer.

Transient Absorption. Pump pulses were generated by pumping an OPA (OPerA Solo, Coherent) with the output of a 1 kHz Ti:sapphire amplifier (Legend Elite HE+, Coherent). UV pump pulses were generated by two successive doubling stages of the OPA output. A white light continuum probe was prepared by focusing the 800 nm Ti:sapphire output onto a 3 mm thick rotating CaF$_2$ window. Before white light generation, a polarizer was set to rotate the probe beam to the magic angle with respect to the pump to eliminate rotational diffusion effects. The pump beam was modulated at 500 Hz using an optical chopper. The probe was detected using a 320 mm focal length spectrometer with 150 g/mm gratings (Horiba iHR320) and a 1340 × 100 CCD array (Princeton Instruments Pixis). A balanced detection scheme was employed to eliminate noise due to fluctuations in the probe spectrum. The probe arm of the apparatus was split with a 50/50 beamsplitter into two arms: sample and reference. The beam in the sample arm was directed to the sample and focused and overlapped with the pump beam. The reference arm was passed through the sample but in a location that is not pumped. Both probe beams were detected by displacing their focal planes on the CCD such that the sample and reference beams are contained by the top half and bottom half of the CCD respectively. The signal resulting from the sample beam contains the transient absorption and fluctuations due to the instability of the probe. The signal resulting from the reference beam only contains the fluctuations. The reported transient absorption signals were

calculated by subtracting the reference signal from the sample signal. The focal spot size diameters for the pump and probe were 29 and 95 μm, respectively. Cross correlations of the pump and probe were collected using the nonresonant response of the flow cell filled with deionized (DI) water (Figures S40, S41, and S42). The width of this nonresonant response is shorter than the 1 ps time step-sizes used in these experiments which we report as our effective time resolution. Aqueous solutions of ∼0.3 mM for each compound were prepared. The pH of each solution was adjusted with NaOH and HCl. The samples were flowed through a fused quartz flow cell with a 0.1 mm path length. Each sample was pumped near its $^1(\pi,\pi^*)$ absorption maximum with pulse energies of 300−500 nJ. NH$_2$Q was pumped at 333 nm, MeOQ was pumped at 310 nm, and Q, ClQ, BrQ, and CNQ were pumped at 287 nm. Samples were pumped at several different powers to check that the signals reported were linear in pump power (Figures S43, S44, S45, and S46).

◼ RESULTS AND DISCUSSION

The set of molecules investigated showed a surprisingly wide variety of spectral features and relaxation mechanisms despite their chemical similarity. We discovered cases of singlet state proton transfer (NH$_2$Q, MeOQ) and triplet state proton transfer (Q, CNQ). Additionally, we have evidence that proton transfer does not occur in two of the compounds (ClQ, BrQ). As a result of the complexity of this set of data, each compound must be treated individually. We first outline our guidelines for identifying the relevant chemical species involved in the analysis of kinetics. Then we describe the dynamics of each compound in order of increasing complexity. A summary of the findings on these excited state dynamics is shown in Table 1 where the compounds are ordered by increasing Hammett parameter of the substituents.

Identification of Transient Chemical Species. Formally, all transient absorption (TA) spectra contain a sum of three components: excited state absorption (ESA) (positive ΔA), stimulated emission (SE) (negative ΔA), and ground state bleach (GSB) (negative ΔA). These features often overlap spectrally, and in some cases can be separated by comparison to steady state data and curve fitting. We use the following spectroscopic signatures and assumptions for interpretation of our ultrafast data.

Protonated Form/Acid. We can identify the TA spectrum of the acid species by forcing protonation in the ground state with a pH two units lower than the pK_a and exciting the acid species. We will refer to this as the acid-form spectrum. In all cases but one (CNQ), this spectrum does not have significant time evolution, meaning it relaxes to its minimum on the order of our time resolution (∼1 ps). In most cases the transient SE band matches the steady state fluorescence spectrum. We display the fluorescence spectrum inverted and scaled for easier comparison to the SE peaks.

Deprotonated Form/Base. We can identify the TA spectrum of the base form by forcing deprotonation with a pH two units greater than the pK_a and exciting the base species. We assign the transient spectrum immediately after excitation to the base form. This assumes that proton transfer is always slower than our time resolution of 1 ps. Studies of similar compounds typically report proton transfer times in the 10−1000 ps range.[1] Direct comparison to steady state emission, as is done for the acids, is not possible for the deprotonated forms
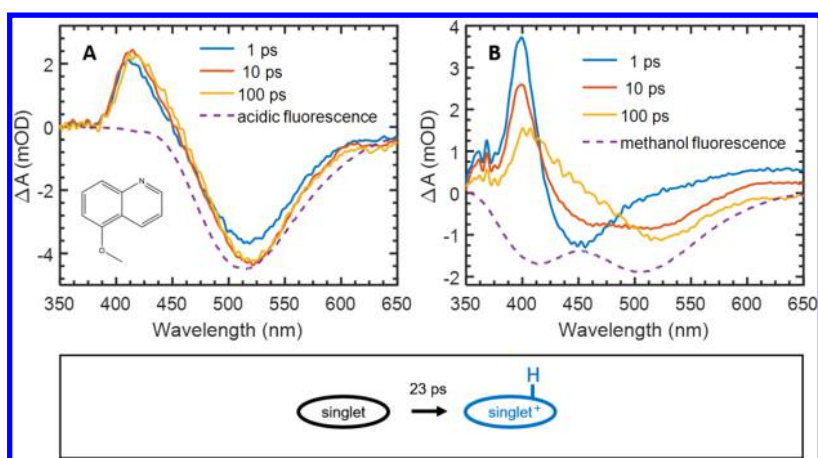
Figure 1. 5-Methoxyquinoline transient absorption in water: (A) TA spectra at pH 3.0 (solid), steady state fluorescence in acidic water displayed inverted and scaled (dashed); (B) TA spectra at pH 7.0 (solid), steady state fluorescence in methanol displayed inverted and scaled (dashed).
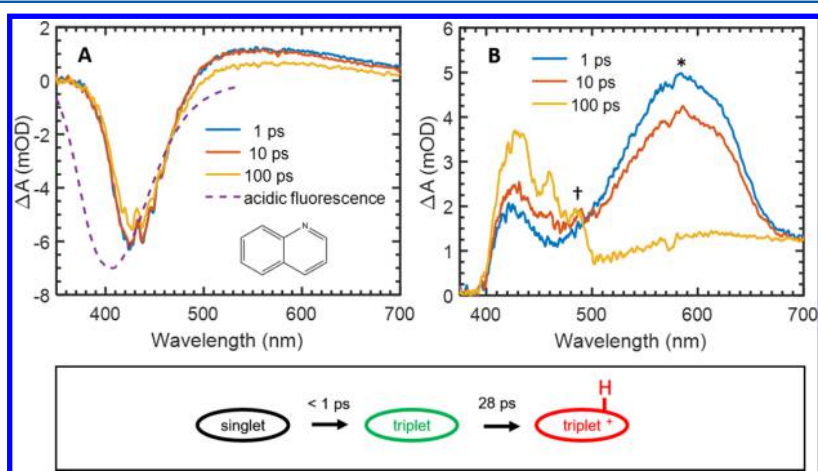

Figure 2. Quinoline transient absorption in water: (A) TA spectra at pH 2.4 (solid), steady state fluorescence in acidic water displayed inverted and scaled (dashed); (B) TA spectra at pH 7.0. As explained in the text, these TA spectra are evidence for rapid triplet formation, which is consistent with the lack of steady state fluorescence. Triplet−triplet absorption energies used to construct the state diagram in Figure 6 are marked with † and *.

because their quantum yield for fluorescence in water is quite low.

Singlet State. Although a singlet state is always initially excited, ISC may be ultrafast (<1 ps) in heteroaromatic systems.[28] Therefore, the first spectrum in a time series must have its spin state identified. The presence of a SE band, ideally one that matches steady state fluorescence data, is indicative of a singlet state. In cases where the overall signal is positive due to overlap with ESA bands, the line shape is fit with a combination of negative and positive Gaussians to extract the SE band.

Triplet State. Excited states of compounds that have low quantum yield in steady state measurements, no transient SE signal, but do have transient ESA, are assigned to triplet states. The presence of these features can be determined if fitting the line shape can be done with only positive Gaussian functions.

Chemical Exchange. An isosbestic point in a series of time ordered spectra is evidence of population transfer between two chemically distinct species. When an isosbestic point is present, the time-ordered spectra contain a band (either ESA or SE) which decreases in magnitude while another band simultaneously increases. The time constant associated with this process is extracted using singular value decomposition

(SVD)[29,30] of the full 2D data set and curve fitting with exponentials. If there is evidence for chemical exchange between singlet and triplet states, the time constant is assigned to intersystem crossing (ISC). If exchange is between base and acid forms, it is assigned to proton transfer (PT).

Finally, our data suggest rapid internal conversion (<1 ps) within both the singlet and triplet manifolds, consistent with Kasha's rule. For this reason we do not concern ourselves with chemical exchange between S_n and S_1 or T_n and T_1.

We found that there is no discernible trend in relaxation mechanism with respect to Hammett parameter. For this reason, we have chosen to describe the dynamics of each compound in order of increasing complexity of explanation to facilitate the reader's understanding. A summary of these findings is provided later in Table 1. The full two-dimensional data sets for all compounds are included in the Supporting Information, ordered by increasing Hammett parameter. We present spectral slices of this data throughout the paper.

5-Methoxyquinoline. In 5-methoxyquinoline (MeOQ) we observe evidence for singlet state photobasicity. Fluorescence measurements in protic and aprotic solvents show two distinct emission wavelengths (Figure S12). These distinct spectral features will serve as markers for the protonation state of the
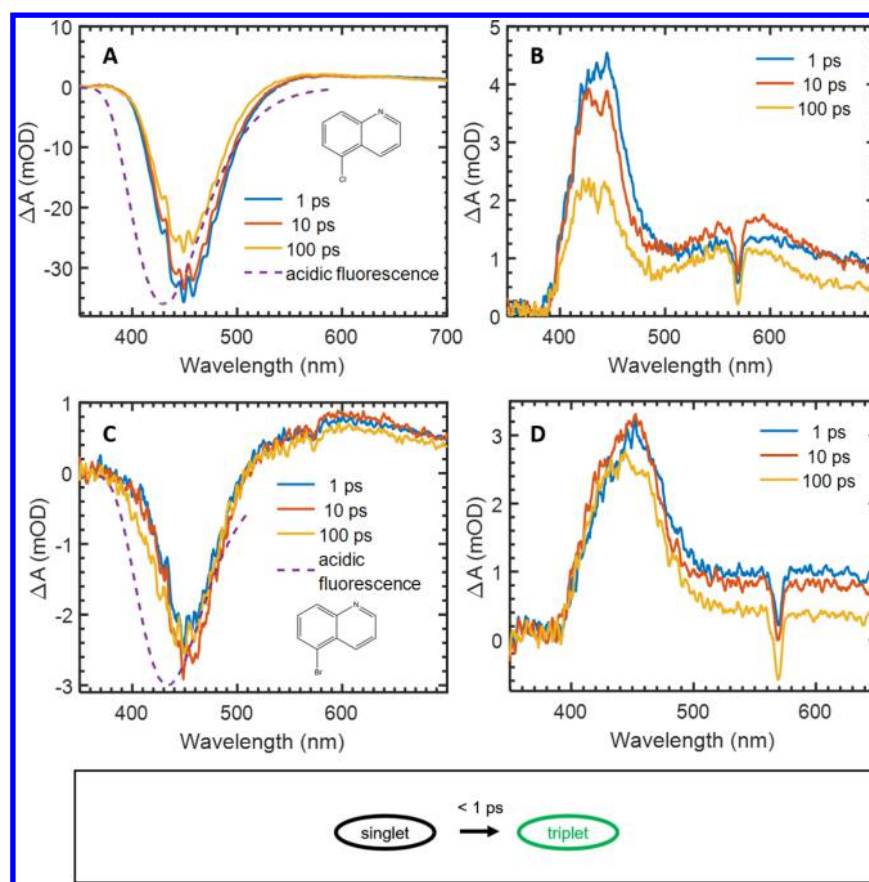
Figure 3. Halogenated quinoline transient absorption in water: (A) 5-chloroquinoline TA at pH 1.8 (solid), steady state fluorescence in acidic water displayed inverted and scaled (dashed); (B) 5-chloroquinoline TA at pH 5.3; (C) 5-bromoquinoline TA at pH 1.9 (solid), steady state fluorescence in acidic water displayed inverted and scaled (dashed); (D) 5-bromoquinoline TA at pH 5.3. The sharp feature at 570 nm is an artifact from pump scatter.

emitting molecule. In chloroform MeOQ emits at 388 nm and in aqueous solution at a pH below its pK_a it emits at 512 nm. Solvatochromism alone cannot account for this difference. Therefore, we assign the two emission wavelengths to the deprotonated and protonated forms, respectively. In aqueous solution with pH greater than the pK_a, the molecule still emits near 512 nm. This implies that even though the molecule is deprotonated in the ground state, it captures a proton from water in the excited state and emits in the acidic form. To further prove this point, we measured the emission spectra in methanol, which is harder to deprotonate than water. Interestingly, we observed two distinct peaks, one near 415 nm, and another near 506 nm (shown inverted in Figure 1B). This indicates that only a fraction of the excited MeOQ population captures protons from methanol and the rest remains in the deprotonated form. Although this observation provides evidence for excited state proton transfer, our ultrafast TA data described below measure the kinetics and provides further supporting evidence.

The acid-form transient absorption spectrum (Figure 1A) contains an SE band that matches the fluorescence spectrum and shows neither significant relaxation nor chemical exchange. This indicates that when the protonated molecule is excited, it remains in the protonated form in the excited state without any significant dynamics.

When the base form is pumped (Figure 1B), two SE bands, similar to the dual fluorescence in methanol, exchange with one another. The wavelength mismatch between the SE and the fluorescence bands is due to solvatochromism and the overlapping ESA feature. Decomposition of the overlapping ESA and SE features is shown in Figure S15. From the spectral signatures above, the isosbestic points at 410 and 480 nm are assigned to chemical exchange between acid and base forms. The time constant associated with this interconversion is 23 ps and is assigned to proton capture from water in the singlet state.

Quinoline. In quinoline we observe evidence for triplet state photobasicity. The acid-form spectrum shows the same behavior as that of MeOQ: there is minimal relaxation on the time scale probed, SE that coincides with the fluorescence maximum (Figure 2A), and no evidence for chemical exchange. There is a nearly 25 nm wavelength mismatch between the SE and fluorescence that may be due to the presence of an underlying ESA band near 400 nm similar to that observed in the spectrum of MeOQ. This ESA band, most likely $^1L_a \rightarrow {}^1(n,\pi^*)$, may also be responsible for the sharp features in the TA that look like a vibronic progression. When the base form is excited, in stark contrast to MeOQ, the transient spectra only contain ESA features (Figure 2B). The absence of SE bands, even at short delay times, suggests rapid triplet formation (ISC) after excitation as discussed earlier under the identification of transient chemical species section. This observation corroborates the low fluorescence quantum yield observed in high pH water. From these observations we assign these ESA bands to triplet–triplet absorption. Principle component analysis shows conversion between two major species within the triplet
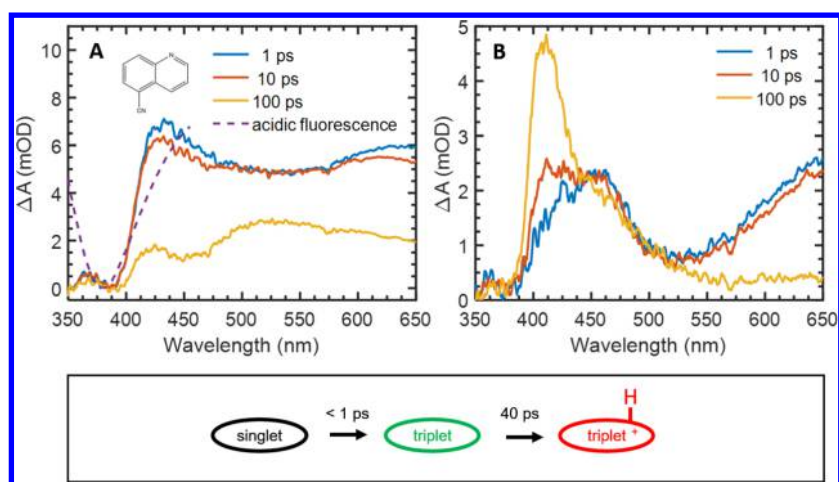
Figure 4. 5-Cyanoquinoline transient absorption in water: (A) pH 1.2; (B) pH 7.0 (B).
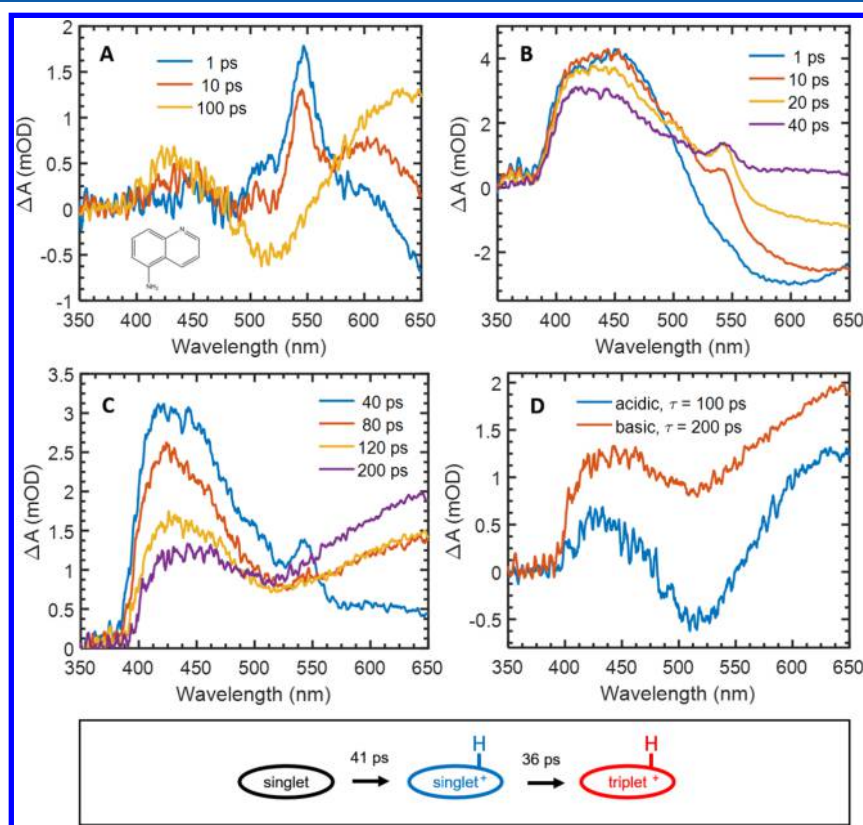

Figure 5. 5-Aminoquinoline transient absorption: (A) pH 3.4; (B) pH 8.2 at early times; (C) pH 8.2 at late times. (D) Transient spectra of acidic and basic solutions at long time delays.

manifold corresponding to the isosbestic point near 500 nm that we plausibly assign to protonated and deprotonated triplet states. The conversion between these two species, i.e., protonated and deprotonated triplets, occurs with a time constant of 28 ps.

5-Chloro- and 5-Bromoquinoline. In 5-chloro- and 5-bromoquinoline we have evidence that proton transfer does not occur. The acid-form spectra of the halogenated compounds (Figure 3A,C) were similar to those of quinoline and MeOQ, showing minimal relaxation, an SE band that roughly matches the fluorescence, and no chemical exchange. The TA spectra of the excited base form (Figure 3B,D) show only ESA features, suggesting rapid ISC similar to the case for quinoline. However,

they do not show a clear isosbestic point. Population transfer, i.e., chemical exchange, between species could not be identified via principle component analysis. This suggests that no proton transfer occurs after triplet formation. Ultrafast proton transfer that is less than 1 ps is unlikely, given the longer time-constants observed for other photobases in both the current study and elsewhere.[1]

5-Cyanoquinoline. In 5-cyanoquinoline we observe evidence for triplet state photobasicity. In acidic media 5-cyanoquinoline has a large fluorescence quantum yield. However, the acid-form spectrum contains many broad positive ESA features (Figure 4A). The fluorescence roughly matches a feature that is concave up, although it is difficult to separate it

from the ESA features even with curve fitting. There are some dynamics present in the ESA features. However, we are hesitant to assign them on the basis of the complex shape and poor fits obtained.

The excited base form transient spectra (Figure 4B) look similar to that of quinoline: one ESA band at early times that exchanges for another ESA band at later times. Just as in quinoline, proton transfer occurs after initial rapid triplet formation. This is consistent with the poor fluorescence quantum yield for CNQ in the base form. The exchange process within the triplet manifold has a time constant of 40 ps and, as is the case for quinoline, is assigned to triplet state proton capture.

5-Aminoquinoline. For 5-aminoquinoline we have evidence for singlet state proton transfer and further relaxation to the triplet state. Unlike the other compounds investigated, NH_2Q has low fluorescence quantum yield in both acidic and basic conditions. The acidic transient spectra (Figure 5A) show dynamics and evidence for chemical exchange: an isosbestic point at 570 nm. At early times the TA contains a sharp ESA feature at 545 nm and a broad SE band on the red edge of the spectrum, indicating that it is a singlet. These features disappear and become two ESA bands, indicating the formation of a triplet. The time constant associated with this exchange is 36 ps and is assigned to ISC of the protonated form.

Under basic conditions we initially see an SE band on the red edge of the spectrum, indicating a singlet state (Figure 5B). Within 40 ps, the sharp ESA band at 545 nm that was also present in the singlet acidic spectrum appears, indicating proton capture by the singlet state. From this point onward, the time evolution of the spectra seems to be similar to that of the photoexcited acidic form. This is evidenced by chemical exchange at later times (Figure 5C), although the isosbestic point is not very well-defined. Furthermore, the final spectrum at $t = 200$ ps is similar to the acid-form spectrum, a protonated triplet. The slight mismatch in shapes of the final spectra (Figure 5D) is due to a small negative band at 515 nm in the acid-form spectrum, which is emission from contaminating MeOQ as justified in the Supporting Information (Figure S9). The above description suggests a two-step process, in which the singlet state first captures a proton and then intersystem crosses to a triplet state. Decomposition of these data required two components. The first component has a time constant of 41 ps and is assigned to singlet state proton transfer. The second component had a time constant of 27 ps and is assigned to ISC. However, the fit obtained for this second component is poor, resulting in a large uncertainty for this time constant (Figure S8). For this reason, we report the 36 ps time constant obtained from the acidic solution measurements as the ISC time constant in this two-step mechanism.

Electronic States in Quinoline and Quinolinium Ion. From the data in the previous section we realize that the excited state dynamics of the quinoline family is diverse and complicated. There is no obvious trend in kinetics with respect to the substituents' Hammett parameters, in contrast to proton transfer in the 1-naphthol photoacid family reported previously.[27] Furthermore, triplet states are often involved. These observations necessitate that we examine the data in the context of the electronic structure of quinoline and quinolinium ion. Quinoline's first two singlet states are both of (π,π^*) character and are commonly referred to by the notation introduced by Platt[31] as ^1L_a and ^1L_b. The ^1L_a state exhibits atom-centered electron density and has a broad absorption,

Table 1. Ultrafast Dynamics of 5-Substituted Quinolines in Their Base and Cationic Forms Ordered by Hammett σ_p Parameter

R	σ_p	species	τ (ps)	assignment
NH_2	−0.66	acid	36	ISC
NH_2	−0.66	base	41	singlet PT
OCH_3	−0.27	base	23	singlet PT
H	0.00	base	28	triplet PT
Cl	0.23	base	N/A	N/A
Br	0.23	base	N/A	N/A
CN	0.66	base	40	triplet PT

whereas the ^1L_b state exhibits bond-centered electron density and has sharp vibronic features. We discussed the effects of substitution and protonation on the energies of these states in our previous work, which is briefly summarized below. Though the energy of ^1L_b is relatively independent of protonation and substituent, ^1L_a is very sensitive to both. Protonation lowers the energy of ^1L_a by 3200 cm^{-1} in quinoline. Substitution with electron-donating groups in the 5 position also lowers the energy of ^1L_a. Additionally, the energy of ^1L_a has been shown to be influenced by hydrogen bonding and other solvent interactions.[32]

The third electronic absorption is of $^1(n,\pi^*)$ character and is deeper in the UV near 230 nm. This state is also red-shifted by substitution of electron-donating groups (Figure S39). Although this $^1(n,\pi^*)$ state is relatively far into the UV, its corresponding triplet, $^3(n,\pi^*)$, is approximately degenerate with the ^1L_a and ^1L_b states. For that reason, it is important to consider its involvement in intersystem crossing. This is particularly important because the El-Sayed rule predicts that states with different orbital angular momenta can have fast rates of ISC.[23,33,34]

Given the sensitivity of ^1L_a and $^3(n,\pi^*)$ to the solvent environment and substituent, we expect that the ordering of states may switch and thus qualitatively change the observed dynamics. In Figure 6, we show the estimated ordering of states for quinoline. The ordering of states in the figure is based on the known properties in quinoline in the literature, our work, and several assumptions and approximations, which are summarized in Table 2. The energies for ^1L_a and ^1L_b are the
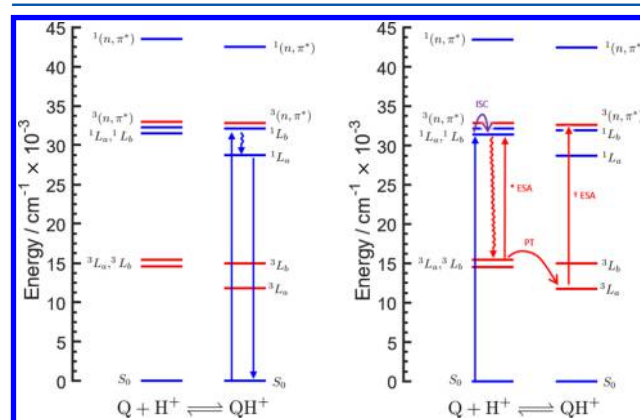

Figure 6. Approximate singlet (blue) and triplet (red) state ordering in quinoline and quinolinium ion in water. Degenerate levels are drawn with slight displacement for clarity. Proposed mechanisms for fluorescence of quinolinium (left) and triplet photobasicity of quinoline (right).

Table 2. Approximate Energy Levels of Quinoline and Quinolinium Ion in Water

index	species	state	E (cm^{-1})	method of assignment
1	base	$^1(\text{n},\pi^*)$	43 500	absorption (Figure S18)
2	base	$^1\text{L}_\text{a}$	31 900	absorption/emission, Table 1 in ref 14
3	base	$^1\text{L}_\text{b}$	31 900	absorption, Table 1 in ref 14
4	base	$^3(\text{n},\pi^*)$	32 100	[5] + 17100 cm^{-1} ($T-T$ absorption, * in Figure 2B)
5	base	$^3\text{L}_\text{b}$	15 000	room temperature phosphorescence, Figure 3 in ref 35
6	base	$^3\text{L}_\text{a}$	15 000	assumed degenerate with [5]
7	acid	$^1(\text{n},\pi^*)$	42 500	absorption (Figure S18)
8	acid	$^3(\text{n},\pi^*)$	32 400	[12] + 20600 cm^{-1} ($T-T$ absorption, † in Figure 2B)
9	acid	$^1\text{L}_\text{b}$	31 900	absorption, Table 1 from ref 14
10	acid	$^1\text{L}_\text{a}$	28 700	absorption/emission, Table 1 in ref 14
11	acid	$^3\text{L}_\text{b}$	15 000	assumed degenerate with [5]
12	acid	$^3\text{L}_\text{a}$	11 800	assumed [11] − [12] is equal to [9] − [10], i.e., protonation shifts $^3\text{L}_\text{a}$ by the same as $^1\text{L}_\text{a}$.

0−0 transitions from our previous work.[14] The $^1(\text{n},\pi^*)$ energy were taken as the UV absorption maximum (Figure S18). The assumptions associated with assigning the triplet states are discussed in detail below.

We used the lowest vibronic peak from the room temperature cyclodextrin matrix phosphorescence as $^3\text{L}_\text{b}$.[35] It has been shown that the cyclodextrin environment is nonpolar, and the $^1\text{L}_\text{b}$ state does not undergo a significant solvatochromatic shift.[36] Therefore, it is reasonable to use the cyclodextrin encapsulated quinoline $^1\text{L}_\text{b}$ state energy in our diagram. We used ESA peaks in our ultrafast data (Figure 2, denoted by * and †) and assigned them to triplet−triplet absorptions. Soon after photoexcitation of the deprotonated form of quinoline (t = 1 ps), the peak of the ESA band is at 585 nm. We assign this process to an excited state absorption within the triplet manifold. The gap within the triplet states of the base form involved in ESA in Figure 6 is determined by these data. The ESA band in the TA spectra moves to a higher energy of 490 nm after proton transfer. Similarly, we assign the gap between the $^3\text{L}_\text{a}$ and $^3(\text{n},\pi^*)$ in quinolinium on the basis of these data. The lowering of the $^3\text{L}_\text{a}$ state with respect to the $^3\text{L}_\text{b}$ state upon protonation by approximately 3200 cm^{-1} as shown in Figure 6 is justified on the basis of comparison to the singlet states. There is experimental evidence in the absorption spectra confirming lowering of $^1\text{L}_\text{a}$ with respect to $^1\text{L}_\text{b}$ upon protonation. However, this assumption may not be quantitative, because it is observed by others that ΔpK_a for triplets tends to be smaller than it is for singlets in other molecules.[11] Therefore, the shift of $^3\text{L}_\text{a}$ with respect to $^3\text{L}_\text{b}$, may be considered a theoretical maximum.

Observed Kinetics. Figure 6 shows our estimates for the ordering of the energy levels in quinoline and illustrates the experimental ultrafast observations. In acidic solution, quinoline becomes protonated in the ground state and has a high quantum yield of fluorescence. This suggests that internal conversion is faster than intersystem crossing (ISC). Therefore, quinoline relaxes to $^1\text{L}_\text{a}$, below the nearest triplet state, and ISC is prevented (Figure 6, left). In basic solution, deprotonated quinoline is excited into a dense manifold of states allowing ISC to occur, thus quenching the fluorescence. After internal

conversion in the triplet manifold, proton transfer can take place (Figure 6, right).

We cannot estimate the ordering of the states for the other compounds without phosphorescence data. However, we propose that each derivative has an electronic structure qualitatively similar to that of quinoline, albeit perturbed by the substituents. Absorption spectra of the quinoline family show that small increases in the electron-donating capability of the substituents red shift the $^1\text{L}_\text{a}$[14] and $^1(\text{n},\pi^*)$ states (Figure S39). It is plausible to assume that the energy of the $^3(\text{n},\pi^*)$ is also lowered by electron-donating substituents. The intersystem crossing rate is therefore extremely sensitive to substitution in the 5 position. This sensitivity may be the reason this family of photobases contains such diverse photophysics for compounds that are chemically very similar.

Previously, we had compared the ΔpK_a values of 5-R-quinoline photobases to those of the structurally similar 5-R-1-naphthol photoacid family.[14,27] This analysis showed that the singlet pK_a^* values in quinoline photobases followed a Hammett relation, analogous to the 1-naphthol family. In the 1-naphthol system the rates of proton transfer as a function of substituent Hammett parameter were shown to follow Marcus theory applied to proton transfer. In the quinoline family, however, there is no trend of rates with respect to substituents' Hammett parameter (Table 1).

There are four compounds, Q, ClQ, BrQ, and CNQ, that do not establish singlet excited state protic equilibrium and relax by other pathways. Strictly speaking, their acid−base energy gap should no longer be referred to as a singlet pK_a^* value, because pK_a is formally a thermodynamic concept that presumes chemical equilibrium has been reached. However, the values of these energy gaps, as calculated with the Förster cycle, remain valid.

The lack of proton transfer in the halogenated compounds is not easily explained in terms of the heavy atom effect or halogen bonding.[37] One may speculate that a large barrier in the excited state would lead to such observations. Theoretical investigations on the rate of intersystem crossing and excited state potential energy surfaces would help to elucidate these observations.

Qualitatively, we see that two categories arise: in molecules with electron-withdrawing substituents ISC is faster than 1 ps and in molecules with electron-donating substituents ISC either is slow or is not observed. Here, special attention must be given to 5-aminoquinoline, which undergoes proton transfer in a singlet state but ultimately relaxes to a protonated triplet state. It has been reported that 7-hydroxyquinoline forms water wires between the alcohol substituent and heterocyclic nitrogen.[38,39] Similarly, we suspect that solvent−solute hydrogen bonding in AQ may complicate its dynamics. Because these effects are not captured by the Hammett parameter, it may be the reason that AQ does not properly fit into the above two categories. Ultrafast experiments on 5-(piperidin-1-yl)quinoline may be useful in separating the electron-donating and hydrogen-bonding effects in this system, as have been done for 3-(piperidin-1-yl)quinoline.[40]

■ CONCLUSION

Proton capture dynamics in the 5-R-quinoline family of photobases, where R = {NH$_2$, CH$_3$O, H, Cl, Br, CN}, were investigated. The pK_a^* values calculated on the basis of singlet states for these compounds are changed in a linear fashion according to the Hammett equation. However, such a

relationship is not observed in the dynamics of proton capture due to the involvement of triplet states. MeOQ undergoes singlet state proton capture with a time constant of 23 ps and $\Delta pK_a = +10$. Quinoline and CNQ undergo triplet PT with time constants of 28 and 40 ps, respectively. In the halogenated compounds there is evidence that proton transfer does not occur. Finally, NH_2Q appears to undergo singlet state proton transfer and subsequent intersystem crossing with time constants of 41 and 36 ps, respectively. Although we cannot accurately estimate the ΔpK_a of triplet states without phosphorescence measurements, we expect them to be smaller than the reported singlet ΔpK_a values, as is common for other photobases and photoacids.[2,11] In analogy to their photoacid counterparts, these large pK_a jumps, especially in long-lived triplet states, may find applications in photomediated catalytic processes that require removal of protons. These diverse dynamics, which change qualitatively with a small perturbation on the molecular framework, could benefit significantly from further theoretical investigation with particular attention to details such as state-ordering, intersystem crossing, solvation, and hydrogen bonding.

ASSOCIATED CONTENT

Ⓢ Supporting Information

The Supporting Information is available free of charge on the ACS Publications website at DOI: 10.1021/acs.jpca.7b04512.

> Collection of absorption, emission, and transient absorption spectra and fits for the set of compounds studied (spot size measurements, cross correlations, and power dependence) (PDF)

AUTHOR INFORMATION

Corresponding Author

*J. M. Dawlaty. E-mail: dawlaty@usc.edu 213-740-9337.

ORCID Ⓞ

Jahan M. Dawlaty: 0000-0001-5218-847X

Notes

The authors declare no competing financial interest.

ACKNOWLEDGMENTS

REFERENCES

(1) Arnaut, L. G.; Formosinho, S. J. Excited-state Proton Transfer Reactions I. Fundamentals and Intermolecular Reactions. *J. Photochem. Photobiol., A* **1993**, *75*, 1−20.

(2) Ireland, J. F.; Wyatt, P. A. H. Acid-Base Properties of Electronically Excited States of Organic Molecules. *Adv. Phys. Org. Chem.* **1976**, *12*, 131−221.

(3) Tolbert, L. M.; Solntev, K. M. Excited-State Proton Transfer: From Constrained Systems to "Super" Photoacids to Superfast Proton Transfer. *Acc. Chem. Res.* **2002**, *35*, 19−27.

(4) Pines, D.; Nibbering, E. T. J.; Pines, E. Monitoring the Microscopic Molecular Mechanisms of Proton Transfer in Acid-base Reactions in Aqueous Solutions. *Isr. J. Chem.* **2015**, *55*, 1240−1251.

(5) Simkovitch, R.; Karton-Lifshin, N.; Shomer, S.; Shabat, D.; Huppert, D. Ultrafast Excited-state Proton Transfer to the Solvent Occurs on a Hundred-Femtosecond Time-scale. *J. Phys. Chem. A* **2013**, *117*, 3405−3413.

(6) Dempsey, J. L.; Winkler, J. R.; Gray, H. B. Mechanism of H_2 Evolution from a Photogenerated Hydridocobaloxime. *J. Am. Chem. Soc.* **2010**, *132*, 16774−16776.

(7) Abbruzzetti, S.; Crema, E.; Masino, L.; Vecli, A.; Viappiani, C.; Small, J. R.; Libertini, L. J.; Small, E. W. Fast Events in Protein Folding: Structural Volume Changes Accompanying the Early Events in the N–>I Transition of Apomyoglobin Induced by Ultrafast Ph Jump. *Biophys. J.* **2000**, *78*, 405−415.

(8) Peretz-Soroka, H.; Pevzner, A.; Davidi, G.; Naddaka, V.; Kwiat, M.; Huppert, D.; Patolsky, F. Manipulating and Monitoring On-Surface Biological Reactions by Light-Triggered Local pH Alterations. *Nano Lett.* **2015**, *15*, 4758−4768.

(9) Anton, M. F.; Moomaw, W. R. Luminescence and Hydrogen Bonding in Quinoline and Isoquinoline. *J. Chem. Phys.* **1977**, *66*, 1808−1818.

(10) Schulman, S. G.; Capomacchia, A. C. Dual Fluorescence of the Quinolinium Cation. *J. Am. Chem. Soc.* **1973**, *95*, 2763−2766.

(11) Kellmann, A.; Lion, Y. Acid-Base Equilibria of the Excited Singlet and Triplet States and the Semi-Reduced Form of Acridine Orange. *Photochem. Photobiol.* **1979**, *29*, 217−222.

(12) Favaro, G.; Mazzucato, U.; Masetti, F. Excited State Reactivity of Aza Aromatics. I. Basicity of 3-styrylpyridines in the First Excited Singlet State. *J. Phys. Chem.* **1973**, *77*, 601−604.

(13) Vogt, S.; Schulman, S. G. Reversible Proton Transfer in Photoexcited Xanthone. *Chem. Phys. Lett.* **1983**, *97*, 450−3.

(14) Driscoll, E. W.; Hunt, J. R.; Dawlaty, J. M. Photobasicity in Quinolines: Origin and Tunability via the Substituents' Hammett Parameters. *J. Phys. Chem. Lett.* **2016**, *7*, 2093−2099.

(15) Poizat, O.; Bardez, E.; Buntinx, G.; Alain, V. Picosecond Dynamics of the Photoexcited 6-Methoxyquinoline and 6-Hydroxyquinoline Molecules in Solution. *J. Phys. Chem. A* **2004**, *108*, 1873−1880.

(16) Munitz, N.; Avital, Y.; Pines, D.; Nibbering, E. T. J.; Pines, E. Cation-Enhanced Deprotonation of Water by a Strong Photobase. *Isr. J. Chem.* **2009**, *49*, 261−272.

(17) Park, S.-Y.; Ghosh, P.; Park, S. O.; Lee, Y. M.; Kwak, S. K.; Kwon, O.-H. Origin of Ultraweak Fluorescence of 8-hydroxyquinoline in Water: Photoinduced Ultrafast Proton Transfer. *RSC Adv.* **2016**, *6*, 9812−9821.

(18) Charton, M. The Application of the Hammett Equation to Polycyclic Aromatic Sets. I. Quinolines and Isoquinolines. *J. Org. Chem.* **1965**, *30*, 3341−3345.

(19) Hansch, C.; Leo, a.; Taft, R. W. A Survey of Hammett Substituent Constants and Resonance and Field Parameters. *Chem. Rev.* **1991**, *91*, 165−195.

(20) Förster, T. Elektrolytische Dissoziation Angeregter Moleküle. *Zeitschrift für Elektrochemie und angewandte physikalische Chemie* **1950**, *54*, 42−46.

(21) Weller, A. Fast Reactions of Excited Molecules. *Progress in Reaction Kinetics and Mechanism* **1961**, *1*, 187−214.

(22) Kasha, M. Characterization of Electronic Transitions in Complex Molecules. *Discuss. Faraday Soc.* **1950**, *9*, 14−19.

(23) El-Sayed, M. A. Spin-Orbit Coupling and the Radiationless Processes in Nitrogen Heterocyclics. *J. Chem. Phys.* **1963**, *38*, 2834−2838.

(24) Hadley, S. G. Direct Determination of Singlet → Triplet Intersystem Crossing Quantum Yield. II. Quinoline, Isoquinoline, and Quinoxaline. *J. Phys. Chem.* **1971**, *75*, 2083−2086.

(25) Anton, M. F.; Nicol, M. Dynamics of the Alcohol-Induced Fluorescence of Quinoline. *J. Lumin.* **1979**, *18*, 131−134.

(26) Komura, A.; Uchida, K.; Yagi, M.; Higuchi, J. Electron Spin Resonance and Phosphorescence of Quinoline, Isoquinoline and Their Protonated Cations in the Phosphorescent Triplet States. *J. Photochem. Photobiol., A* **1988**, *42*, 293−300.

(27) Prémont-Schwarz, M.; Barak, T.; Pines, D.; Nibbering, E. T. J.; Pines, E. Ultrafast Excited-State Proton-Transfer Reaction of 1-Naphthol-3,6-Disulfonate and Several 5-Substituted 1-Naphthol Derivatives. *J. Phys. Chem. B* **2013**, *117*, 4594−4603.

(28) Eisenhart, T. T.; Dempsey, J. L. Photo-induced Proton-Coupled Electron Transfer Reactions of Acridine Orange: Comprehensive Spectral and Kinetics Analysis I. Experimental Methods. *J. Am. Chem. Soc.* **2014**, *136*, 12221−12224.

(29) Shrager, R. I.; Hendler, R. W. Titration of Individual Components in a Mixture with Resolution of Difference Spectra, pKs, and Redox Transitions. *Anal. Chem.* **1982**, *54*, 1147−1152.

(30) Henry, E.; Hofrichter, J. Singular Value Decomposition: Application to Analysis of Experimental Data. *Methods Enzymol.* **1992**, *210*, 129−192.

(31) Platt, J. R. Classification of Spectra of Cata-Condensed Hydrocarbons. *J. Chem. Phys.* **1949**, *17*, 484.

(32) Osada, M.; Toyoshima, K.; Mizutani, T.; Minami, K.; Watanabe, M.; Adschiri, T.; Arai, K. Estimation of the Degree of Hydrogen Bonding Between Quinoline and Water by Ultraviolet-visible Absorbance Spectroscopy in Sub- and Supercritical Water. *J. Chem. Phys.* **2003**, *118*, 4573−4577.

(33) Lim, E. C.; Yu, J. M. H. Vibronic Spin−Orbit Interactions in Heteroaromatic Molecules. I. Polycyclic Monoazines. *J. Chem. Phys.* **1967**, *47*, 3270−3275.

(34) Baba, M. Intersystem Crossing in the $^1n\pi^*$ and $^1\pi\pi^*$ States. *J. Phys. Chem. A* **2011**, *115*, 9514−9519.

(35) Scypinski, S.; Love, L. J. C. Cyclodextrin-Induced Room-Temperature Phosphorescence of Nitrogen-Heterocycles and Bridged Biphenyls. *Anal. Chem.* **1984**, *56*, 331−336.

(36) Santo, M.; Cattana, R.; Silber, J. J. Hydrogen Bonding and Dipolar Interactions Between Quinolines and Organic Solvents. Nuclear Magnetic Resonance and Ultraviolet-visible Spectroscopic Studies. *Spectrochim. Acta, Part A* **2001**, *57*, 1541−1553.

(37) Politzer, P.; Lane, P.; Concha, M. C.; Ma, Y.; Murray, J. S. An Overview of Halogen Bonding. *J. Mol. Model.* **2007**, *13*, 305−311.

(38) Park, S.-Y.; Kim, B.; Lee, Y.-S.; Kwon, O.-H.; Jang, D.-J. Triple Proton Transfer of Excited 7-hydroxyquinoline along a Hydrogen-Bonded Water Chain in Ethers: Secondary Solvent Effect on the Reaction Rate. *Photochemical & photobiological sciences: Official journal of the European Photochemistry Association and the European Society for Photobiology* **2009**, *8*, 1611−7.

(39) Hoffmann, F.; Ekimova, M.; Bekçioğlu-Neff, G.; Nibbering, E. T. J.; Sebastiani, D. Combined Experimental and Theoretical Study of the Transient IR Spectroscopy of 7-Hydroxyquinoline in the First Electronically Excited Singlet State. *J. Phys. Chem. A* **2016**, *120*, 9378−9389.

(40) Singh, A. K.; Ghosh, S.; Kancherla, R.; Datta, A. Engineering the Excited State Dynamics of 3-Aminoquinoline by Chemical Modification and Temperature. *J. Phys. Chem. B* **2016**, *120*, 12920−12927.